

GFF
Volume 143, part 4
pages 391-405

A Scandinavian Journal of Earth Sciences

GFF

ISSN: (Print) (Online) Journal homepage: <https://www.tandfonline.com/loi/sgff20>

Rock fracturing by subglacial hydraulic jacking in basement rocks, eastern Sweden: the role of beam failure

Maarten Krabbendam, Romesh Palamakumbura, Christian Arnhardt & Adrian Hall

To cite this article: Maarten Krabbendam, Romesh Palamakumbura, Christian Arnhardt & Adrian Hall (2021) Rock fracturing by subglacial hydraulic jacking in basement rocks, eastern Sweden: the role of beam failure, GFF, 143:4, 390-405, DOI: [10.1080/11035897.2021.1939776](https://doi.org/10.1080/11035897.2021.1939776)

To link to this article: <https://doi.org/10.1080/11035897.2021.1939776>



© 2021 British Geological Survey, A component body of the UKRI. BGS (c) UKRI. Published by Informa UK Limited, trading as Taylor & Francis Group



Published online: 15 Jul 2021.



Submit your article to this journal [↗](#)



Article views: 573



View related articles [↗](#)





View Crossmark data [↗](#)



Citing articles: 1 View citing articles [↗](#)

Rock fracturing by subglacial hydraulic jacking in basement rocks, eastern Sweden: the role of beam failure

Maarten Krabbendam ^a, Romesh Palamakumbura^a, Christian Arnhardt^b and Adrian Hall ^c

^aBritish Geological Survey, The Lyell Centre, Research Avenue South, Edinburgh UK; ^bBritish Geological Survey, Environmental Science Centre, Nicker Hill, Keyworth, Nottingham, UK; ^cDepartment of Physical Geography, Stockholm University, Stockholm, Sweden

ABSTRACT

Dense networks of dilated fractures occur locally in the upper 5–15 m of bedrock in basement gneisses in eastern Sweden. Near Forsmark, pre-existing sub-horizontal fractures have been jacked open and filled with water-lain sediment, likely during the latest Weichselian glaciation. Despite extensive previous research, it is uncertain whether subglacial hydraulic jacking led to the generation of new fractures, in addition to reactivation of pre-existing ones. Re-analysis of historic photos from excavations near the Forsmark power plant indicates formation of two types of new fracture. Firstly, rock fragments were broken off the main fracture surfaces as existing fractures were jacked open. Secondly, fracture analysis shows that whilst few subvertical fractures occur above tight sub-horizontal fractures, a higher density of vertical fractures occurs above dilated sub-horizontal fractures, suggesting new formation. We apply a model of beam failure theory, borrowed from structural engineering, to constrain potential new fracture generation, using assumptions based on measured water pressure fluctuations from beneath the Greenland Ice Sheet. This modelling shows that beam failure is a plausible mechanism for the generation of new vertical fractures during a subglacial water fluctuation cycle under a range of realistic glaciological conditions. This implies that hydraulic jacking can result in further *in situ* disruption and brecciation of the shallow rock mass, decreasing the rock mass strength and increasing its hydraulic conductivity. Altogether, hydraulic jacking of existing fractures and the formation of new vertical fractures results in effective subglacial mechanical weathering of the shallow rock mass.

ARTICLE HISTORY

Received 13 January 2021
Accepted 25 May 2021

KEYWORDS

Basement fractures;
hydraulic jacking;
overpressure; glaciation;
fracture density; brecciation;
mechanical weathering

Introduction

The near-surface formation of fracture networks in basement rocks represents a form of mechanical weathering of the shallow rock mass. In non-glacial environments, this is recognised as a common phenomenon with implications for the evolution of the “critical zone”, relevant for groundwater use, engineering properties, as well as the long-term weathering and erosion of basement terrains (Brantley et al. 2007; Holbrook et al. 2019; Collins et al. 2020). In subglacial environments, the formation or growth of rock fractures has been investigated in theoretical papers (e.g., Morland & Morris 1977; Iverson 1991; Hallet 1996; Zoet et al. 2013), and has been documented in sedimentary rocks (Phillips et al. 2013), but convincing observational evidence for the subglacial formation of new fractures in basement rocks is sparse.

In basement gneiss of eastern Sweden (Fig. 1), dense networks of dilated fractures are locally abundant in the upper 5–15 m of bedrock (Fig. 2A). Excavations related to the construction of the Forsmark nuclear power plant in the 1970s, as well as later test-excavations, revealed sub-horizontal fractures, up to 170 m long in section, that are dilated and filled by 1–80 cm of laminated silt and sand (Stephansson & Ericsson 1975; Carlsson 1979; Leijon 2005; Forsberg et al. 2007). The dilation of subhorizontal fractures and their sediment fill suggest that hydraulic jacking by overpressured water occurred during Pleistocene glaciations. Studies on fracture coatings, such as

chlorite, epidote and iron staining, indicate that most fractures were first formed during the Precambrian and Palaeozoic (Sandström et al. 2008; 2009), so that Pleistocene hydraulic jacking largely involved the reactivation of pre-existing fractures. However, some vertical fractures appear free of coatings and may have formed during Pleistocene glaciation. Despite extensive studies on various aspects of bedrock fractures at Forsmark (e.g., Carlsson 1979; Follin et al. 2007; Forsberg et al. 2007; Martin 2007; Moon et al. 2020), it is not clear if some new (vertical) fractures in the shallow subsurface were generated during hydraulic jacking by subglacial meltwater.

Origin of shallow fractures in basement rocks

An increase in fracture density in the near surface is observed in many basement terrains composed of massive rock; associated subhorizontal fractures are termed sheeting joints (also: exfoliation joints). Their near-surface occurrence suggests a component of “unloading”, combined with horizontal stresses (Jahns 1943; Twidale 1973; Ziegler et al. 2013); Martel (2017) showed that topographic curvature as well as ground water pressure facilitate the formation of sheeting joints. Sheeting joints are known to form near the Earth’s surface during the *first exhumation* of massive rock masses, for instance in young granite domes (Sierra Nevada, USA, e.g., Martel 2017), or during development of deep glacial troughs



Figure 1. Location map of Uppsala and Gävleborgs counties (län), eastern Sweden, with visited quarries and section indicated. DTM © Lantmäteriet. Boulder spreads after Geological Survey of Sweden (SGU) map database. Figure © Svensk Kärnbränslehantering AB.

(e.g., in the Swiss Alps; Ziegler et al. 2013). Shallow rock masses that have only experienced a single exhumation episode are dominated by subhorizontal sheeting joints with only few vertical connecting fractures. As an example, the Dharwar Craton in south India has been exhumed by weathering and erosion more or less continuously since the Cretaceous, driven by rift-shoulder uplift, as India separated from other Gondwana continents (e.g., Gunnell 1998). Sheeting joints in felsic orthogneiss near Mysore (Fig. 2B) are well developed down to c. 12 m, are tens of metres long, and form a broadly anastomosing network, with very few connecting vertical fractures. The rock slabs delineated by the joints have a length: height ratio of >10:1.

In eastern Sweden, the first exhumation of the basement rocks occurred during the Mesoproterozoic, followed by several cycles of burial and re-exhumation (Stephens 2010; Japsen et al. 2016). These events did not result in deep erosion of the basement (Hall et al. 2019a, b), so that earlier formed shallow fracture networks were not destroyed by erosion but instead were re-activated. The shallow basement in Sweden has a more complex loading/unloading history than first-exhumation

rock masses, and the resulting fracture networks are more complex (compare Fig. 2A and B). This implies that vertical, near-surface, fractures in eastern Sweden may be younger, secondary features, not primarily related to exhumation-related sheeting jointing, and possibly generated subglacially below the latest Weichselian ice sheet.

Setting and previous work

Most of eastern Sweden consists of crystalline basement, comprising various felsic gneisses with subordinate amphibolite, formed between 1.9 and 1.8 Ga (e.g., Stephens 2010). The rocks cooled and were partly exhumed soon thereafter, after which all deformation occurred in the brittle regime (Sandström et al. 2008). In east-central Sweden, the first near-surface exhumation of the basement occurred in the Mesoproterozoic, prior to burial by “Jotnian sandstone”. In the early Neoproterozoic and Palaeozoic at least two further cycles of loading and unloading occurred during deposition and removal of Sveconorwegian and Caledonian foreland basins; near surface exhumation occurred prior to burial by Cambro-Ordovician sediments (Stephens 2010; Japsen et al. 2016; Hall et al. 2019b). The basement along the western shore of the Baltic Sea was likely then re-exposed only during the Pleistocene (Hall et al. 2019a; Hall & Van Boeckel 2020). Further repeated loading and unloading occurred beneath 1–3 km thick Pleistocene ice sheets (Carlsson & Olsson 1982a; Svensk Kärnbränslehantering 2010). A dominant horizontal NW-SE compressive stress system affects the rock mass in eastern Sweden; close to the surface these horizontal stresses exceed the vertical stresses (Carlsson & Olsson 1982a, b; Martin 2007).

Near Forsmark, older, Precambrian ductile structures of the gneisses show a number of steeply dipping, anastomosing NW-SE orientated shear zones that separate kilometre-wide lenses of less deformed rocks (e.g., Follin et al. 2007; Stephens 2010). Most long subhorizontal fractures occur within these less-deformed lenses, consistent with observations elsewhere that sheeting joints preferentially occur in massive rocks (e.g., Jahns 1943; Martel 2017). There is a general upward increase in fracture density (Svensk Kärnbränslehantering 2013), but in particular in the top 10 m (Carlsson 1979). The shallow fracture networks and their sediment fill were studied by Stephansson & Ericsson (1975) and Carlsson (1979) at large construction excavations (Fig. 3A, B), and by Leijon (2005) and Forsberg et al. (2007) in later, smaller test excavations (Fig. 3C). The dominant fracture system is formed by long subhorizontal fractures, connected with shorter, subvertical fractures. In excavated sections, subhorizontal fractures had much larger aperture (10–100 mm) than steep fractures (typically <1–2 mm; Carlsson 1979; Carlsson & Olsson 1982b). This compares with much smaller apertures of 0.5–5 mm below 15 m (Carlsson & Olsson 1978; Svensk Kärnbränslehantering 2013).

Fractures are commonly coated with minerals such as chlorite, epidote, corrensite, quartz, calcite and hematite. Detailed analysis has shown that these were formed during at least three phases, the first two during Proterozoic, and the last during the Palaeozoic; most fractures were thus formed well before Quaternary glaciation (Sandström et al. 2008; 2009; 2010; Sandström & Tullborg 2009). Fractures were re-opened

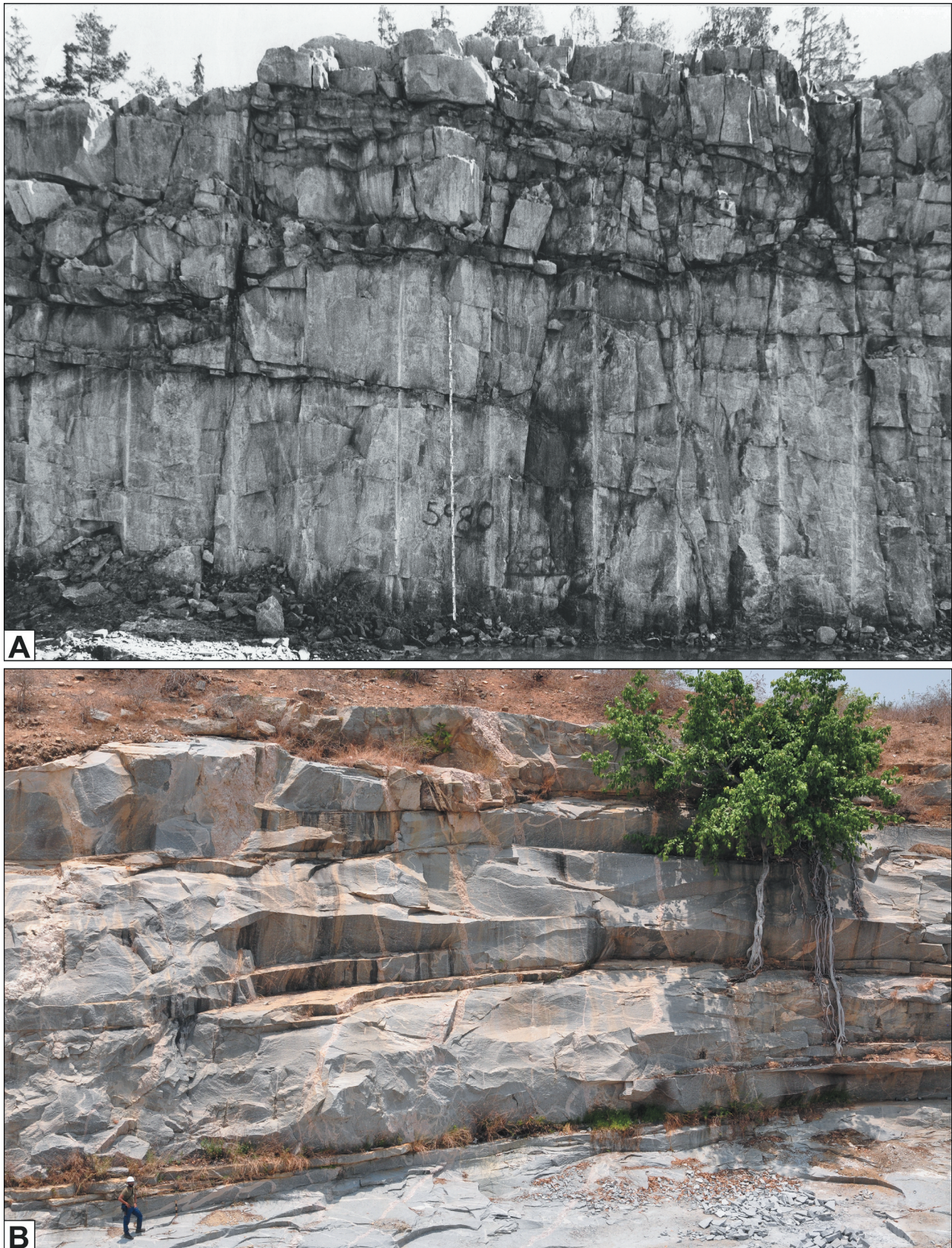


Figure 2. Comparison of complex (eastern Sweden) and simple (south India) shallow fracture networks in basement. **A.** Fracture network in the shallow rock mass, eastern Sweden, showing a dense network of subhorizontal and subvertical fractures: the top part of the section shows brecciation. Several subhorizontal fractures are dilated and are filled by sediment. Photo from excavation for the cooling water intake canal, Forsmark nuclear power plant (Carlson 1979; Fig. 39). The stick is 4 m long. Photo: Göran Hansson, © Svensk Kärnbränslehantering AB. **B.** Sheeting joints in felsic orthogneiss, Peninsular Gneiss, Western Dharwar craton. Disused quarry, north of Mysore, Karnataka, south India [E 76°.5953; N 12°.5381]. Person and scale bar in bottom left corner. Photo: © British Geological Survey.

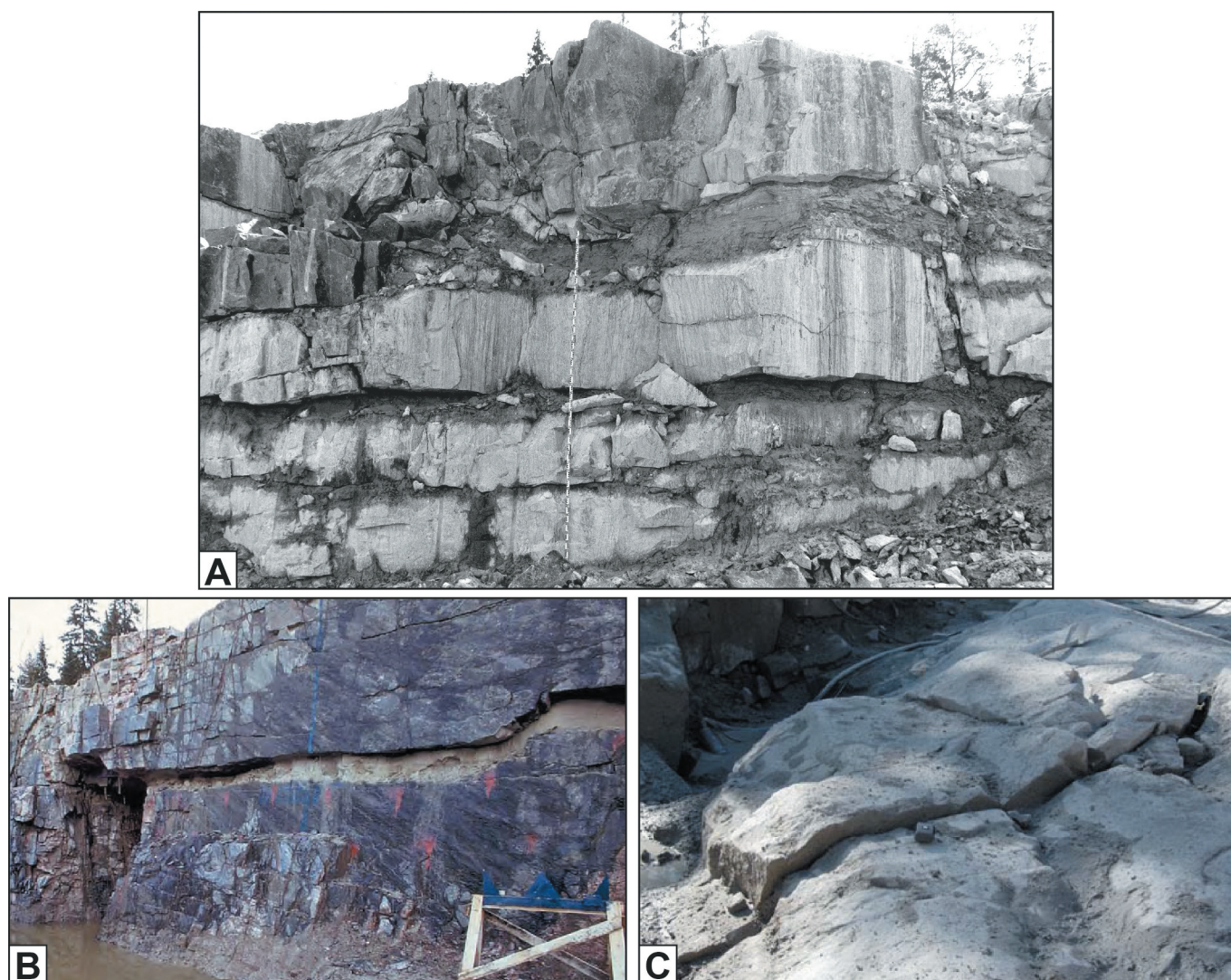


Figure 3. Bedrock with open fractures and sediment fill, east Sweden. **A.** Open fractures with sediment fill in excavation for the nuclear power plant cooling water intake canal, Forsmark. The stick is 4 m long. (Carlson 1979, Fig. 39; Photo: Göran Hansson). **B.** Open fractures with sediment-fill in excavation for the nuclear power plant construction, Forsmark (Leijon 2005; Figures. 5–1). Fracture is c. 50 cm wide. Photo: Göran Hansson. **C.** Jacking, showing displacement of abraded surface, temporary excavation AFM 001364, Forsmark (Forsberg et al. 2007; Figure B5). Figure © Svensk Kärnbränslehantering AB.

to depths of 500 m under the presently prevailing stress regime (Moon et al. 2020). Carlsson (1979) provided detailed counts on the number of coated vs uncoated fractures for different joint sets: most fractures (75–90%) are coated with chlorite – and thus are old features; however, up to 25% of subvertical E-W trending joints in the power plant excavations at Forsmark were uncoated (Carlsson 1979). Deeper in bedrock, only very few (<5%) of fractures are uncoated (Claesson Liljedahl et al. 2011). Other temporary excavations in the Forsmark area also record uncoated vertical fractures (Hermanson et al. 2003; Leijon 2005; Lagerbäck et al. 2005). These reports suggest the possibility that uncoated vertical fractures at shallow depths at Forsmark are new fractures.

Although open fractures at Forsmark occur at considerable (>100 m) depth (Follin et al. 2007; Svensk

Kärnbränslehantering 2013), sediment-filled fractures (Figs. 2A, 3) are common only in the upper 5–15 m (Carlsson 1979; Leijon 2005). Sediment fill in bedrock fractures consists mainly of silt, with minor sand and diamicton, and some rock fragments (Carlsson 1979; Leijon 2005). The silt-sand fills show locally laminations indicating deposition by flowing water (Stephansson & Ericsson 1975; Carlsson 1979; Leijon 2005). Microfossil and pollen content of the silt sediment in the fractures is similar to that of nearby till deposits (Stephansson & Ericsson 1975; Robertsson 2004), consistent with sourcing of the sediment from till at the ice-bed interface. Compression tests on the sediment fill suggest it was subjected to pre-consolidated load of 3400–3900 kPa (Carlsson & Olsson 1976; Carlsson 1979), and compressed by considerable effective stress, requiring substantial ice thickness.

Stephansson & Ericsson (1975) envisaged fracture dilation by freeze-thaw action during an interglacial, and subsequent sediment fill during ice cover. This model requires the dilated fractures to remain open for a long time, which is difficult to reconcile with the observation of sharp edges of differentially uplifted but abraded rock blocks (Fig. 3c) near Forsmark (Forssberg et al. 2007). In contrast, Pusch et al. (1990) envisaged a scenario wherein hydraulic jacking occurred proglacially, with overpressure created by ice retreating over a frozen bed, resulting in strong hydraulic gradient between the ice sheet and the foreland, leading to overpressure in the glacial foreland. This model relies on a permafrost layer functioning as an aquitard, to retain high water pressures in the glacial foreland. This model is at odds with the high pre-consolidation loads as documented by Carlsson & Olsson (1976) and other various strands of evidence (Hall et al. 2020) that indicate that hydraulic jacking occurred subglacially, rather than proglacially.

Potential groundwater overpressure conditions in the bedrock below Forsmark have been studied and discussed extensively (e.g., Talbot 1990, 1999, 2014; Hökmark et al. 2010; Lönnqvist & Hökmark 2013; Hökmark & Lönnqvist 2014). The normal hydraulic gradient of a sloping ice front (e.g., Boulton et al. 1993) may lead to overpressure in a marginal or proglacial setting, in particular if the water is “locked up” below a low conductivity layer, like permafrost. However, no strong water pressure fluctuations are expected from these mechanisms. In contrast, in the ablation zone of the western Greenland Ice Sheet pressure measurements in boreholes (with ice thickness between 150–800 m) have shown strongly fluctuating water pressures on a seasonal and daily basis at the ice-bed interface (Andrews et al. 2014; Claesson Liljedahl et al. 2016; Wright et al. 2016; Harper et al. 2019). Water pressures in boreholes varies from 80 to 110% of overburden pressure. In moulins, in regions that are well-connected to the bed, Andrews et al. (2014) measured water-pressure fluctuations between 60 and near 100% overburden pressure on a daily basis during the melt season.

Hall et al. (2020) suggested that such repeated overpressure events operating beneath the latest Weichselian Fennoscandian ice sheet were responsible for the hydraulic jacking of subhorizontal fractures in eastern Sweden. In addition, they interpreted the jacking of subhorizontal fractures as the first step towards glacial ripping, an erosional process that involves jacking, disintegration and transport, ultimately resulting in boulder spreads that are widespread in lowland Sweden.

The aim of this paper is to test the hypotheses that: (i) some vertical fractures in the shallow basement of eastern Sweden may have been newly generated during and following hydraulic jacking of pre-existing subhorizontal fractures by fluctuating water pressures beneath the latest Pleistocene Fennoscandian Ice Sheet, and (ii) such newly formed vertical fractures contribute to the fracturing of the shallow rock mass and thus constitute an enhanced mode of subglacial mechanical weathering. We re-analyse historic photos from the Forsmark excavations in terms of fracture density for both subhorizontal and subvertical fractures. We then apply classic beam theory borrowed from structural engineering to test if

new vertical fractures can be generated during subglacial water pressure fluctuations.

Methods

To test how representative the Forsmark subhorizontal fractures are for east Sweden, a number of quarries and sections were visited (Fig. 1) and described qualitatively. Historic photos from the canal and test excavations at Forsmark were kindly provided by Svensk Kärnbränslehantering AB (SKB). Many of these photos have an accurate scale (ranging pole). Observations on sediment fill, fracture distribution and brecciation were made from these photos. For further fracture analysis, the historic photos were imported in a GIS and georeferenced against an artificial, but accurately scaled 1 m grid. Fracture networks were digitised from these images, giving a quantified 2D dataset of a vertical section of particular fracture sets (full details of the method in Palamakumbura et al. 2020). Once the fracture networks are captured as lines in a GIS, various statistical operations can be applied to derive data on fracture density or spacing and fracture dip. Fracture density is reported as fracture length divided by surface area, in m^{-1} , or the number of fractures per unit length, also in m^{-1} , following Singhal and Gupta (2010). Fracture spacing is then simply the reciprocal of fracture density, in m. Fracture dilation is identified visually from the photograph and attributed to the corresponding digital fracture trace. For the modelling, we apply classic beam theory from structural engineering, and adapt this for subglacial conditions, explained in that section.

Results – Observations

Variations in shallow fracture networks in eastern Sweden

In the various quarries studied across Uppsala and Gävleborg counties (Fig. 1; Table 1), fracture networks are highly variable in character, fracture density and fracture aperture, and substantial changes can occur over short distances. As an example, in the Uppsala Krossen quarry in granitic gneiss, one section shows subhorizontal fractures with pronounced curvature, connected by steeper fractures (Fig. 4A). The curved subhorizontal fractures are akin to sheeting joints but do not follow the topographic surface (cf. Martel 2017), rather, they terminate against gently dipping fracture zones that separate the different sections (this may be regarded as “pseudo-topography” delineating solid bedrock, which would have the same mechanical effect as true topography in the models of Martel (2017)). An adjacent section, in contrast, shows an orthogonal fracture pattern, with subvertical and subhorizontal fractures (Fig. 4B). A third section is dominated by a “criss-cross” pattern of gently-dipping fractures. None of the fractures is discernibly dilated or jacked. In other quarries such as Alunda Krossen quarry (Fig. 4C), long (>10 m) subvertical fractures dominate, with shorter (<2 m) interconnecting shallow-dipping fractures. Again, no fracture is discernibly jacked.

In contrast, at the Svagberget quarry, SW of Iggesund (Fig. 4D), a more or less continuous sub-horizontal fracture at 4–6 m depth separates coherent bedrock beneath from a rock mass dominated by open fractures, with apertures

Table 1. Fracture characteristics of visited quarries and sections. Grid reference system: Sweref 99. Some names are informal, or refer to the nearest settlement or feature.

Name/location	Fracture pattern	Fracture aperture	Grid ref
North of Iggesund	Steep, inclined and horizontal fractures	Numerous open fractures	E 610,619 N 6,840,553
SW of Iggesund	Multiple fracture sets of steep, inclined and horizontal fractures	Tight; no dilated fractures seen	E 607,738 N 6,834,938
Svagberget Quarry. SW of Iggesund	Orthogonal, dense, long subhorizontal fractures	Numerous open fractures; likely sediment-filled; brecciation in top 6 m	E 605,776 N 6,834,108
“Ironworks”, NW of Gimo	Steep fractures dominate (parallel to gneiss foliation), with short connecting fractures	Tight; no dilated fractures seen	E 666,728 N 6,681,795
Bladåker; quarry	Gently & steeply inclined and vertical fractures	Tight; no dilated fractures seen	E 682,750 N 6,654,741
Alunda Krossen	Steep fractures dominate, with short connecting fractures	Tight; no dilated fractures seen	E 673,853 N 6,662,145
Uppsala Krossen, Sector A	Near orthogonal, with curved subhorizontal fractures; shorter vertical fractures	Tight; no dilated fractures seen	E 656,082 N 6,645,251
Uppsala Krossen, Sector B	Orthogonal, dense, long subhorizontal fracture and vertical fractures	Tight; no dilated fractures seen	E 656,082 N 6,645,251
Uppsala Krossen Sector C	Diamond pattern of inclined fractures	Tight; no dilated fractures seen	E 656,082 N 6,645,251
Norrskedika Quarry	Steep/vertical fractures dominate, with short connecting fractures	Tight; no dilated fractures seen	E 678,830 N 6,688,550
Ballast Quarry, Skyttorp	Multiple fracture sets of steep fractures (parallel to gneiss foliation), inclined and horizontal fractures	Tight; no dilated fractures seen	E 654,931 N 6,662,229
Tönnebro	Dominant subhorizontal/gently inclined fractures; shorter vertical fractures	Tight in most place; open fractures with sediment fill locally.	E 604,990 N 6,770,770
Ljusne quarry	Subhorizontal and gently inclined fractures; shorter vertical fractures	A few open fractures; some brecciation in upper 3 m	E 611,099 N 6,785,493
Karbo quarry	Steep/vertical fractures dominate (parallel to gneiss foliation), with short connecting fractures	Mostly tight; open fractures and brecciation in one small sector	E 618,842 N 6,663,691
Lilla Sandgrund, Outfall Canal section	Subhorizontal and gently inclined fractures; shorter vertical fractures	Tight; no dilated fractures seen	E 675,121 N 6,703,466
Forsmark Excavations	Subhorizontal and gently inclined fractures; shorter vertical fractures	Numerous open fractures; commonly sediment-filled; brecciation in top 1–3 m	(Carlsson 1979)

≥5–10 cm. The upper rock mass is strongly disrupted, even brecciated. Sediment was observed along the main subhorizontal fracture, although close examination was too risky, given the unstable nature of the quarry face.

Although this sample is non-systematic (systematic analysis of fracture distribution in basement terrain with extensive forest and soil cover is not possible), about a quarter of the visited quarries possess open, jacked fractures, close to rock-head, whilst the remainder has tight fractures (Table 1). However, long, dilated sub-horizontal fractures with thick sediment fills (as exemplified by Fig. 3A, B at Forsmark) are comparatively rare.

Additional observations on fracture fill and fracture networks from historic photos

Observations from the historic photos from Forsmark, in addition to those previously reported (Carlsson 1979; Leijon 2005; Forssberg et al. 2007), include the following: In one section (Fig. 5A), crackle and mosaic brecciation (terminology following Morrow 1982) occurs 1 m below the top-rock surface in a zone of closely spaced subhorizontal fractures. In this c. 0.5 m thick zone, the rock mass has clearly been dilated and disrupted to such a degree that blocks have lost coherence, leaving a loose mass of blocks 10–50 cm across, with the creation of substantial void space in between. The rock below appears not to be affected by jacking or dilation. The rock above still shows coherence, but has more vertical fractures than the rather massive rock below the zone. In another

section (Fig. 5B), similar forms of brecciation affect the entire top 3–4 m of bedrock.

In a later test excavation (‘Drill Site 5’; Leijon 2005), a partly sediment-filled fracture shows angular rock fragments (1–20 cm long) that appear to be broken off from the roof of the fracture (Fig. 5C). The rock fragments are partly mixed with fine sediment. On the right (yellow arrows), the rock fragments appear little displaced or rotated, whilst to the left (blue arrow) some rock fragments are substantially rotated and displaced.

In another test excavation (AFM 001264; Forssberg et al. 2007), old vertical fractures, coated with iron oxide are clearly seen (1) on Figure 5D. A possible new fracture is visible on the right, although this could be machine damage during excavation (2). Brecciation into angular rock fragments occurs at two levels. At the upper level (3), brecciation is focused where subvertical and subhorizontal fractures interact, with new formation of short fractures. At the lower level, the subhorizontal fracture shows in detail (Fig. 5E) a sediment fill of silt and sand up to 15 cm thick. The sediment is laminated, but the laminations are disturbed and folded (5). The roof of the fracture is uneven, and the soft-sediment deformation was likely caused by uneven vertical compression during fracture closure, following a water-pressure drop. On the right (6), small (1–2 cm) rock fragments are mixed with sediment. However, some open fractures at the Forsmark excavation show very little brecciation (Fig. 2A). Here a long (>20 m) fracture has opened by c. 50 cm without signs of brecciation and development of new vertical fractures above it; however, this fracture has a continuous fill of silt and sand.

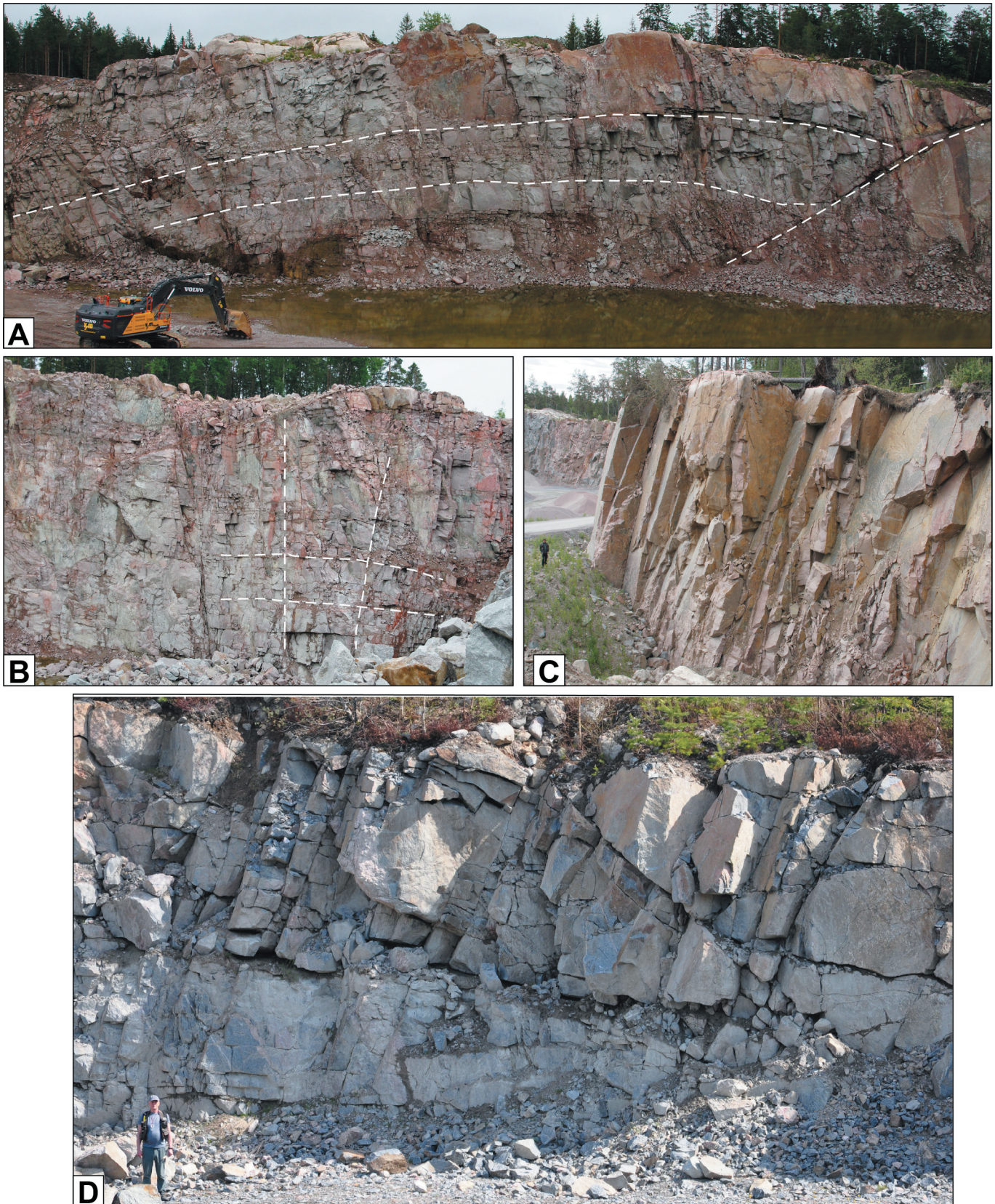


Figure 4. Quarries and sections with different fracture patterns. **A.** Section of Uppsala Krossen quarry [E 656,082; N6645251], with curved “sheeting joints”. **B.** Section of Uppsala Krossen quarry with orthogonal (vertical and horizontal) fractures. **C.** Alunda Krossen quarry [E 673,853; N 6,662,145]; subvertical fractures with chlorite and iron staining. **D.** Open fractures and brecciated bedrock in top 5 m; Svagberget quarry, SW of Iggesund. Disruption from ice moving from left to right. Figure © Svensk Kärnbränslehantering AB.

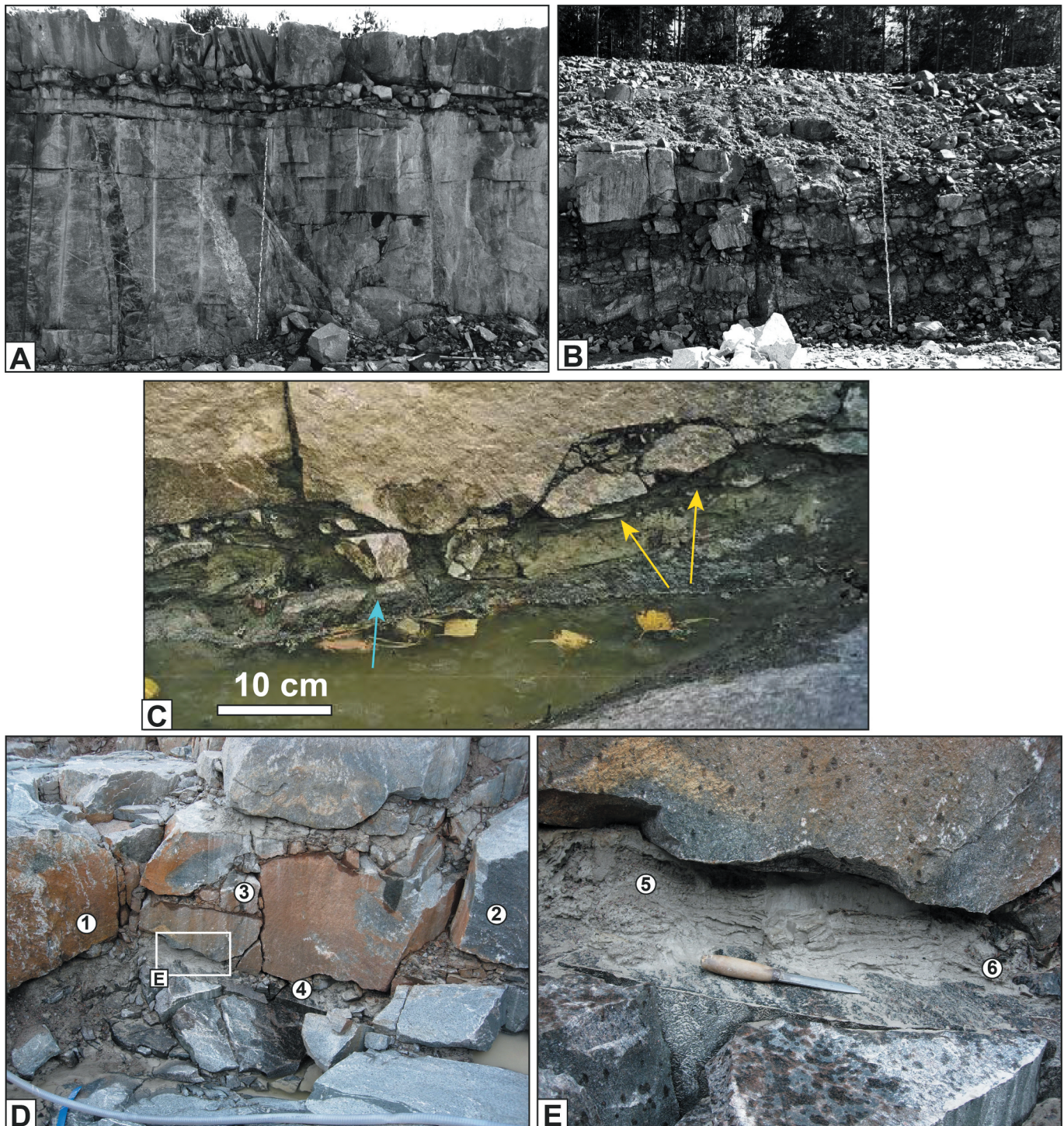


Figure 5. **A.** Layer of brecciated rock, with closely-spaced vertical fractures along a closely-spaced set of subhorizontal fractures, c. 1.5 m below rock surface. Forsmark excavations. **B.** Extensive brecciation in upper 4 m of bedrock. For A, B: The stick is 4 m long. (Carlson 1979; Fig. 39; Photo: Göran Hansson). **C.** Rock fragments detached from roof of dilated subhorizontal fracture. Test excavation at Drill Site 5, Leijon (2005); Photo: Assen Simeonov. **D.** (1) Old, iron-coated fracture; (2) New, uncoated fracture – possibly related to excavation; (3) and (4) brecciation with rock fragments. Test excavation at AFM 001264; Forssberg et al. (2007); Photo: Assen Simeonov. **E.** Detail of sediment-filled subhorizontal fracture in (D), note laminations in sediment; (5) folded lamination; (6) rock fragments mixed with sediment. Test excavation at AFM 001264; Forssberg et al. (2007); Photo: Assen Simeonov. Figure and photos © Svensk Kärnbränslehantering AB.

Fracture analysis from historic photos

Fracture analysis from the historic Forsmark cooling water intake canal photos show a general increase in fracture density towards rock head (Fig. 6), as reported by Carlsson (1979). In our study, we calculated fracture density separately for subvertical and subhorizontal fractures. In two sections

(SKB-003 and SKB-006; Fig. 6A, B), the subvertical and subhorizontal fracture densities increase in tandem, from $<1\text{--}2\text{ m}^{-1}$ at the base of the section to $2\text{--}4\text{ m}^{-1}$ at the top of the sections, with the highest fracture density caused by a concentration of subhorizontal fractures, with numerous subvertical fractures, 1–3 m below rockhead. These two

sections also show the most pronounced dilation along sub-horizontal fractures (blue arrows). A quarry section MK-22 from the Svagberget quarry, SW of Iggesund (Fig. 6H), was also digitised and shows similar high densities for subvertical and subhorizontal fractures. The top 4–6 metres of the section is clearly dilated and the rock mass disrupted. Sediment was observed (from a distance – unstable quarry face) in the subhorizontal fracture that underlies this disrupted rock mass.

In contrast, sections SKB-037, SKB-064 and SKB-031 (Fig. 6C, D, E) show upward increases in subhorizontal fracture density, but only modest increases in the density of subvertical fractures, whereas sections SKB-036 and SKB-057 (Fig. 6F, G) show no increase in subvertical fracture density at all. Fracture dilation is absent in Section SKB-036, and minor in Section SKB-057, SKB-037, SKB-064 and SKB-031.

A nominal or proxy length:height ratio of resultant blocks or slabs (Fig. 7) was calculated by dividing horizontal and

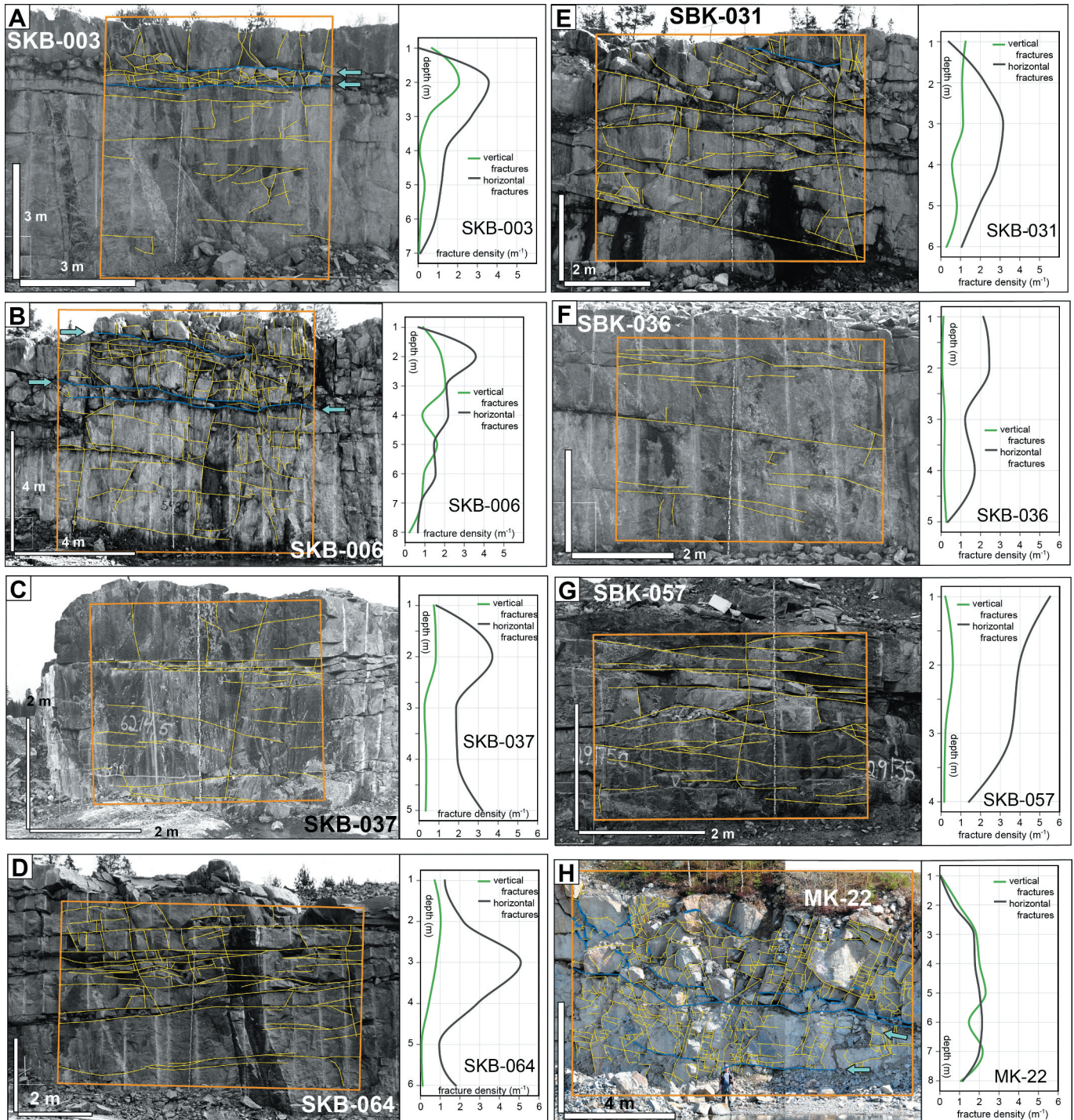


Figure 6. Digitised fracture patterns in the canal excavations at Forsmark (left panels). Blue fractures (with blue arrows) are dilated. Fracture density for subvertical and subhorizontal fractures, against depth (right panels). **A–G** from Forsmark construction excavations – Photos: Göran Hansson; **H**: Svagberget quarry, SW of Iggesund. Figure and photos © Svensk Kärnbränslehantering AB.

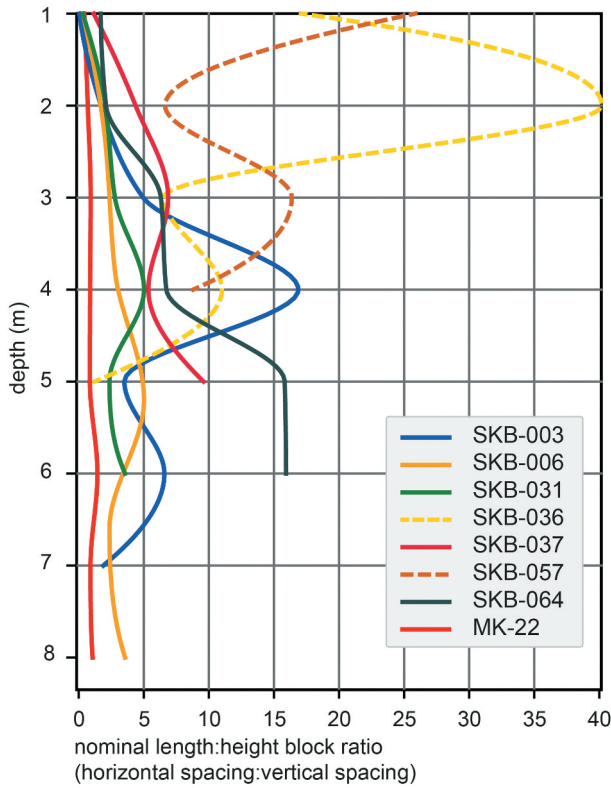


Figure 7. Nominal block length:height ratio, calculated from horizontal fracture spacing: vertical fracture spacing. Figure © Svensk Kärnbränslehantering AB.

vertical fracture spacing (the reciprocal of the horizontal and vertical fracture density). This shows that for section MK22 and SKB-006 the length:height ratio remains below 5 for their entire thickness and that some sections show a marked decrease in length:height towards the top, whilst sections SKB-036 and SKB-057 – which show no dilation at all along subhorizontal fractures – show very long length:height ratios.

Altogether, it appears that an increase in subvertical fracture density in the top few metres of the rock mass is present above dilated subhorizontal fractures, but is absent if subhorizontal fractures are not dilated. This suggests that at least some vertical fractures were formed as a result of dilation of the underlying subhorizontal fractures.

Results – Modelling of beam failure

The modelling here assumes that hydraulic jacking and dilation of subhorizontal fractures were driven by repeated water pressure fluctuations with a daily to seasonal frequency as measured at the base of the Greenland Ice Sheet (Andrews et al. 2014; Claesson Liljedahl et al. 2016; Wright et al. 2016; Harper et al. 2019). Following Wright et al. (2016), relative water pressure is defined here as the fraction of overburden pressure P_w/P_i (where water pressure is P_w , and cryostatic pressure is P_i). If the water pressure equals overburden pressure ($P_w/P_i = 1$), the ice is at (local) flotation, and the effective pressure ($P_w - P_i$) is zero.

Now consider a rectangular slab of rock at the base of an ice sheet, underlain by a transmissive subhorizontal joint (Fig. 8A), that is uplifted (“jacked”) by overpressured

groundwater, by a few centimetres (Fig. 8B). As the water pressure drops, the slab will be lowered again (Fig. 8C). Now consider that the slab will not be lowered back in its exact original place, but is “hanging”, supported at its ends, perhaps by a broken rock fragment (circled in Fig. 8B, C), such as observed in some of the test excavations near Forsmark (Fig. 5C, D, E). The rock slab has now become a bridge or beam (Fig. 8C). This beam is subjected to a bending stress, caused by the load provided by its own weight plus any load of the overlying ice. As the tensile strength of rock is much lower than its compressive strength, when the stresses are too high, the slab or beam may fail in a tensile manner near its base (Fig. 8D). A new subvertical fracture is then formed.

This problem in its simplest form equates to the structural engineering problem of a beam supported at both ends under a uniform distributed load (Fig. 8E). The maximum stress σ_{max} that such a beam is subjected to (compressive at the top and tensile at the base) is given by (EngineeringToolBox 2009):

$$\sigma_{max} = 0.5h_r q_{tot} L^2 / 8I \quad [1]$$

where h_r is the height of the beam, L the length of the beam, q_{tot} is the total load and I is the Area Moment of Inertia.

The Area Moment of Inertia I for a rectangular cross-section is given by (EngineeringToolBox 2008):

$$I = wh_r^3 / 12 \quad [2]$$

so that (taking the width of the beam, $w = 1$):

$$\sigma_{max} = \frac{0.5h_r q_{tot} L^2 12}{8wh_r^3} = \frac{0.75q_{tot} L^2}{h_r^2} \quad [3]$$

The total load q_{tot} is the sum of the load of the overlying rock and the ice, minus the water pressure at the base:

$$q_{tot} = q_r + q_i - P_w = gh_r \rho_r + gh_i \rho_i - P_w \quad [4]$$

where q_r is the load by the rock beam, q_i the load of the ice, P_w the water pressure, g the gravity constant, h_i the thickness of the ice and ρ_i and ρ_r the density of ice and rock respectively.

Since it is convenient to express this in terms of relative water pressure (P_w/P_i), equation [4] is rewritten as (full derivation is given in the Appendix):

$$q_{tot} = gh_r \rho_r + gh_i \rho_i \left(1 - \frac{P_w}{P_i}\right) \quad [5]$$

Thus, the maximum stress at the base of a rock beam as a function of the height and length of the beam and ice thickness and relative water pressure is given by:

$$\sigma_{max} = \frac{0.75 \left[gh_r \rho_r + gh_i \rho_i \left(1 - \frac{P_w}{P_i}\right) \right] L^2}{h_r^2} \quad [6]$$

The maximum length of the beam can then be given as:

$$L = h_r \sqrt{\left[\sigma_{max} / \left(0.75 \left(gh_r \rho_r + gh_i \rho_i \left(1 - \frac{P_w}{P_i}\right) \right) \right) \right]} \quad [7]$$

The tensile yield strength of the felsic granodioritic gneiss at Forsmark is in the order of 10–15 MPa (Glamheden et al. 2007). (In comparison, the compressive strength of the same rocks is in the range of 150–250 MPa). These values are for

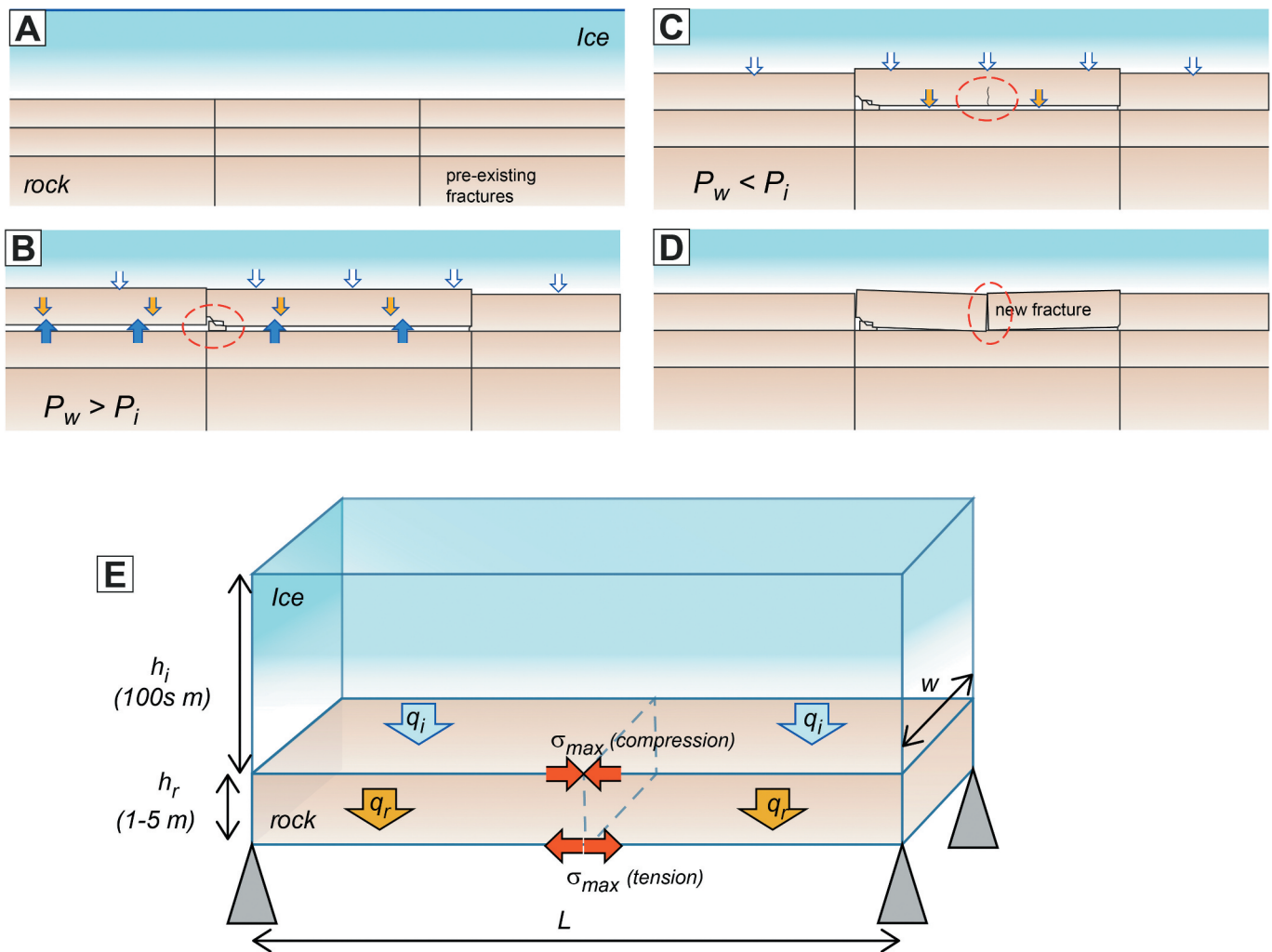


Figure 8. A. Conceptual model of rock overlying rock mass with orthogonal subhorizontal and subvertical fractures. B. During an overpressure event ($P_w > P_i$), rock slabs are lifted upwards. C. As pressure drops, the slabs are lowered again, but not in exactly same position. The imperfectly fitting slab functions as a beam. D. The beam may fail, forming a new fracture. E. Conceptual model of a rock slab as a beam, subjected to a distributed load of rock (q_r) and ice (q_i). Maximum stress σ_{max} is compressional at the top of the beam and tensional at its base. Figure © Svensk Kärnbränslehantering AB.

intact rock without micro fractures or other flaws, so that the tensile strength of 10–15 MPa should be seen as a maximum. In nature, tensile failure is thus likely somewhat lower.

The results (Fig. 9A) show tensile stresses increasing exponentially with the length of the beam, for different scenarios (beam height $h_r = 1$ and 5 m; ice thickness $h_i = 200, 400$ and 600 m; relative water pressure P_w/P_i at 0.8 and 0.9). For instance (left hand line), a 1 m high beam, under 600 m of ice, with a relative water pressure of 0.8, will fail if longer than 3–4 m. Under a wide range of conditions, a 1 m high beam will fail if longer than 2 to 7 m. In contrast, a thick (5 m) beam, under relatively thin ice and high water pressure will not fail at less than 10 m length.

The maximum length for different parameters is plotted against beam height (Fig. 9B), for a fixed tensile strength of 10 MPa. This shows that beams (rock slabs) have the tendency to fracture into short, stubby blocks with a length: height ratio between 4:1 and 3:1. This compares reasonably well with the block length:height ratios as seen in the Forsmark sections, which show ratios $>5:1$ for sections without dilated fractures and $<5:1$ for section with (or above)

dilated subhorizontal fractures (Fig. 8). Overall, the results show that tensile beam failure during low water pressure events (following jacking by high water pressure) is a plausible mechanism for the production of new vertical fractures in long rock slabs.

Discussion

The fracture analysis on the historic photos from the Forsmark excavations shows that:

- dense networks of dilated fractures in the upper 5–10 m of bedrock occur locally in basement gneisses in eastern Sweden;
- In some sections at Forsmark, subvertical fracture density increases upwards in tandem with subhorizontal fracture density, in particular above open, jacked subhorizontal fractures;
- Sections with tight subhorizontal fractures do not show an upward increase in subvertical fracture density.

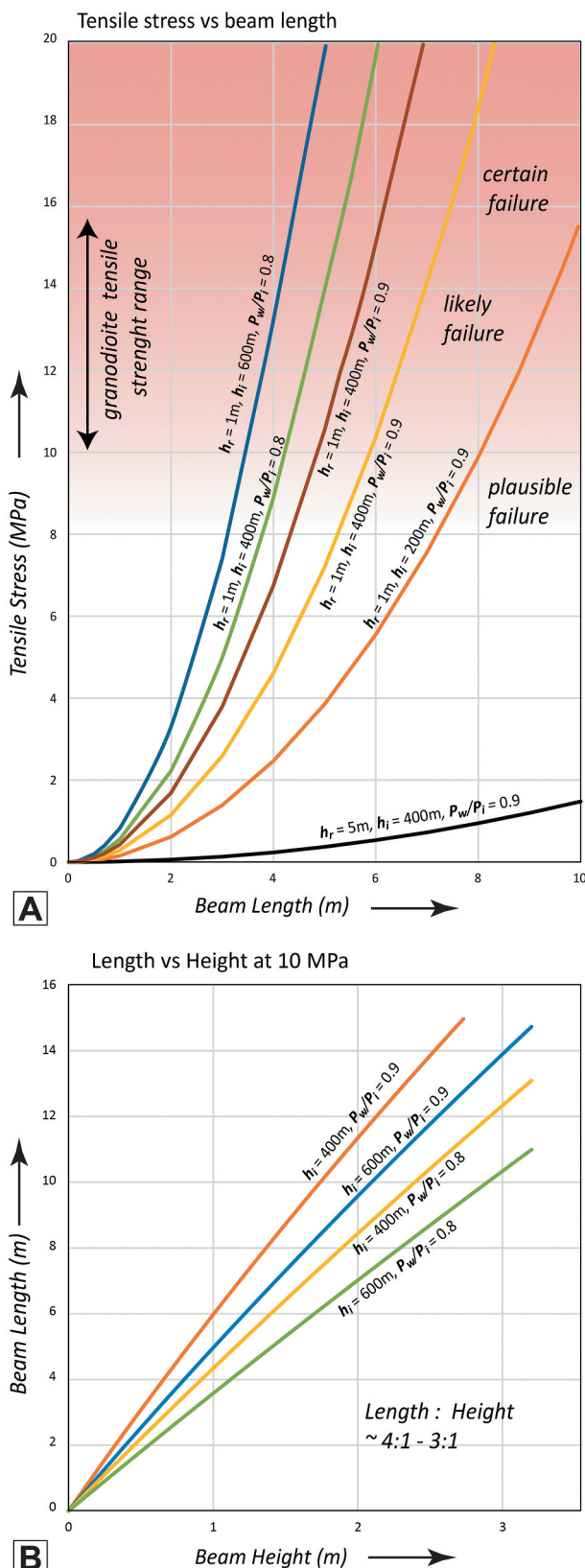


Figure 9. A. Maximum tensile stress (MPa) at the base of a beam against length of beam (L in m) for different values of height or rock beam h_r , ice thicknesses h_i and relative water pressure P_w/P_i . Tensile failure is increasingly likely between 8 and 10 MPa, and certain for stresses > 15 MPa (red shading). B. Maximum length of beam against height of beam at a fixed breaking strength of 10 MPa for different values of ice thickness h_i and P_w/P_i . Figure © Svensk Kärnbränslehantering AB.

This suggests that hydraulic jacking and fracture dilation along subhorizontal fractures locally resulted in the generation of new subvertical fractures. Observations on the historic photos show that the development of angular rock fragments in open sub-horizontal fractures at Forsmark is a common occurrence. This implies that after a high-pressure jacking event, a fracture may remain “jammed” open, leaving some void space. After a water pressure drop and increase in effective pressure, the rock slab above the fracture then functions mechanically like a beam.

The modelling shows it is plausible that, if a rock slab above a dilated or jammed-open fracture functions as a beam, that beam may fail after a hydraulic jacking event as water pressure drops and effective pressure increases. New subvertical fractures and a dense shallow fracture network can thus be generated subglacially. Conversely, the modelling shows that it is *not* plausible for long, intact rock slabs to survive multiple water pressure fluctuations: they have a strong propensity to break up, under a wide range of realistic conditions. This conclusion is supported by the observation of brecciation associated with long subhorizontal fractures near Forsmark and elsewhere. This implies that it is not plausible for long, open fractures to survive a glaciation (cf. Stephansson & Ericsson 1975), and it is more likely that jacking and further disruption occurred during the same glaciation, and likely in a relatively short time frame.

Nevertheless, one such long dilated fracture without additional fracturing or brecciation does occur at Forsmark, but this fracture is filled with 30–50 cm sediment. A solution to this apparent conundrum is that the sediment fill supported the load of the overlying rock slab, like a type of cushion, so that the overlying rock slab did not function like a beam, and thus preventing further break-up of this slab. This is supported by the high pre-consolidation loads measurements by Carlsson (1979). However, this load-bearing role of sediment fill would only be possible if sediment deposition occurred *during* an overpressure cycle. As such this is logic in that an overpressure event is likely to result in vigorous subglacial water flow that can transport sediment into the dilated fractures. Deposition would occur when water velocity drops after peak pressure (e.g., Phillips et al. 2013). The approximate coeval development of dilated fractures and sediment deposition is supported by the observation of mixed rock fragments and sediment fill (Fig. 6).

The generation of dilated, fracture networks in the shallow rock mass at Forsmark thus likely followed the following steps:

- (1) An overpressure event occurs at the ice-bed.
- (2) Water under high-pressure is squeezed into a pre-existing subhorizontal fracture. If water pressure exceeds overburden pressure, the fracture is jacked open, and the overlying rock slab is lifted upwards.
- (3) Locally, rock fragments may break off the roof or the sides of the dilated fracture; this keeps the fracture “jammed” open after water pressure drops;
- (4) Sediment, transported with the water, may be deposited in the dilated fracture, likely soon after peak pressure (e.g., Phillips et al. 2013).

- (5) As water pressure drops, the effective pressure and hence the load of overlying rock and ice increases, and the horizontal fracture tends to close.
- (6) Now there are two possibilities:
 - a. the overlying rock slab functions mechanically like a beam, the combined load of rock and ice breaks the rock slab, and new subvertical fractures are generated,
 - b. If sufficient sediment is available and deposited in the fracture, the sediment may take the load and becomes compressed, but beam failure may not occur;
- (7) Repetition of the above cycle will result in either (i) increasing number of subvertical fractures, resulting in a disrupted rock mass (e.g., Figs. 2A, 3A, 4D), or – more rarely – (ii) very wide (>10 cm) dilated fractures filled with laminated sediment (e.g., Fig. 3B).

The rarity of the wide sediment-filled fractures as seen in Forsmark overlain by *intact* rock suggests that jacking and subsequent beam failure was generally more common than the sediment deposition and cushioning. Sediment availability (presumably sourced from loosely consolidated till at the ice-bed nearby) is in principle independent from overpressure, so it is possible to have a jacking event by water with little sediment. In that case, fracture jacking does occur, but the fracture will not be filled with sediment but with water, and subsequent water-pressure drops can easily lead to beam failure and the creation of new fractures.

Implications

Hydraulic jacking followed by beam failure and the generation of new vertical fractures can create a dense fracture network in the shallow bedrock. This process represents a form of mechanical weathering, operating subglacially. The jacking and fracturing will thus lower the rock mass strength of the shallow bedrock, so that it is easier to erode, be it by plucking or by glacial ripping (Hall et al. 2020). The jacking and fracturing also greatly increases in hydraulic conductivity of the upper rock mass.

There is no *a priori* reason that the same mechanism would not operate in other rocks. In sedimentary rocks, bedding planes may play the role of sheeting joints, in allowing access for water pressure to build up beneath slabs of rock. However, the resultant blocks will, in most rocks, be smaller than in basement rocks, and may well be eroded quickly and turn to till. It is thus possible that jacking and fracturing is a major mechanism of subglacial sediment production in sedimentary rocks (Bukhari et al. 2021).

Finally, the deep overpressure as studied, modelled and discussed widely (Talbot 1990, 1999, 2014; Hökmark et al. 2010; Lönnqvist & Hökmark 2013; Hökmark & Lönnqvist 2014) involves residual pore pressure and relies on the hydraulic gradient of the ice sheet as a whole, combined with low hydraulic conductivity of the bedrock mass. Such low conductivity retards pressure equilibration (“drainage”) during ice advance or retreat and may thus lead to overpressure. We do not think such mechanisms are responsible for the shallow

hydraulic jacking discussed herein because (i) the upper rock mass is characterised by a high conductivity fracture network, that is unlikely to be able to build up sufficient residual pore pressure; (ii) the laminated sediments suggest repeated overpressure events, whilst release of residual pore pressure is likely only as a “one-off” event. Rather, it is likely that the high-frequency, high-magnitude water pressure fluctuations that have been documented to occur beneath the Greenland Ice Sheet (Andrews et al. 2014; Claesson Liljedahl et al. 2016; Wright et al. 2016; Harper et al. 2019) are responsible. Overpressure by such water pressure fluctuations at the ice-bed is limited to about 10% above cryostatic pressure (e.g., Claesson Liljedahl et al. 2016), and can thus only effectively jack open rock to a depth of c. 3% of ice thickness (rock being c. 3 times denser than water). They are thus restricted to the uppermost 10s of metres of the bedrock, consistent with observations. Thus, shallow (<10–30 m) and deep hydraulic jacking (if occurring) are likely driven by very different mechanisms.

Conclusions

Near Forsmark in east-central Sweden, pre-existing subhorizontal fractures have been jacked open and filled with water-lain sediment, creating dense networks of dilated fractures in the upper 5–10 m of basement gneisses. Re-analysis of historic photos from excavations in the shallow rock mass around the Forsmark power plant shows that there is a higher density of vertical fractures above dilated sub-horizontal fractures. Subvertical fractures are less abundant above tight subhorizontal fractures. Rare dilated fractures with thick sediment fill do not show subvertical fractures. Vertical fractures may thus have been newly formed during hydraulic jacking.

It is suggested that the hydraulic jacking is caused by the same high-frequency water pressures fluctuations that have been measured at the base of the Greenland Ice Sheet.

Modelling applying beam theory, borrowed from structural engineering, shows that beam failure is plausible for rock slabs longer than 5–10 m, if they are jacked up and lowered down, under fluctuating water pressures. Beam failure is thus a plausible mechanism for the generation of new vertical fractures above jacked subhorizontal fractures. This explains the dense fracture network (and smaller size of joint-bound blocks) in the shallow subsurface, and explains previous observations that subhorizontal fractures are coated (and hence pre-Quaternary), whereas some subvertical fractures are uncoated and may have developed during the last glaciation. Beam failure modelling also implies it is not plausible that long slabs of rocks are jacked and lowered and remain intact. The exception is if the void space below the jacked slab is filled with sediment, so that the load overlying rock and ice distributed across a wider area of soft sediment. This is only possible if sediment deposition occurred *coevally with the jacking*.

Acknowledgments

Joost Krabbendam is thanked for pointing out (at age 93) the relevance of beam theory. Assen Simeonov and SKB are thanked for providing access to historic photos. Jens-Ove Näslund, Susanne Grigull and Sam Roberson

are thanked for comments on an earlier version of the manuscript. Stefan Bergman and one anonymous reviewer are thanked for constructive comments. MK, RP and CA publish with permission of the Executive Director of BGS.

Funding by Swedish Nuclear Fuel and Waste Management Company (SKB) is gratefully acknowledged.

Disclosure of potential conflicts of interest

No potential conflict of interest was reported by the author(s).

Funding

This work was supported by the by Swedish Nuclear Fuel and Waste Management Company (SKB) [n/a].

ORCID

Maarten Krabbendam  <http://orcid.org/0000-0002-7463-9822>

Adrian Hall  <http://orcid.org/0000-0001-9985-8944>

References

- Andrews, L.C., Catania, G.A., Hoffman, M.J., Gulley, J.D., Lüthi, M.P., Ryser, C., Hawley, R.L., & Neumann, T.A., 2014: Direct observations of evolving subglacial drainage beneath the Greenland Ice Sheet. *Nature* 514, 80–83.
- Boulton, G., Slot, T., Blessing, K., Glasbergen, P., Leijnse, T., & Van Gijssel, K., 1993: Deep circulation of groundwater in overpressured subglacial aquifers and its geological consequences. *Quaternary Science Reviews* 12, 739–745.
- Brantley, S.L., Goldhaber, M.B., & Ragnarsdottir, K.V., 2007: Crossing disciplines and scales to understand the critical zone. *Elements* 3, 307–314.
- Bukhari, S., Eyles, N., Sookhan, S., Mulligan, R., Paulen, R., Maarten, K. M., & Putkinen, N., 2021: Regional subglacial quarrying and abrasion below a paleo ice stream crossing the Shield-Paleozoic boundary of central Canada: the importance of substrate control. *Boreas*. doi:10.1111/bor.12522.
- Carlsson, A., 1979: *Characteristic Features of a Superficial Rock Mass in Southern Sweden*. Unpublished PhD thesis, University of Uppsala.
- Carlsson, A. & Olsson, T., 1976: Joint fillings at Forsmark, Uppland, Sweden: a discussion. *Geologiska Föreningens i Stockholm Förhandlingar* 98, 75–77.
- Carlsson, A. & Olsson, T., 1978: Joint apertures in a pre-Cambrian crystalline rock mass in Sweden. *Bulletin of the International Association of Engineering* 18, 127–130.
- Carlsson, A. & Olsson, T., 1982a: High rock stresses as a consequence of glaciation. *Nature* 298, 739–742.
- Carlsson, A. & Olsson, T., 1982b: Rock bursting phenomena in a superficial rock mass in southern central Sweden. *Rock Mechanics* 15, 99–110.
- Claesson Liljedahl, L., Kontula, A., Harper, J., Näslund, J., Selroos, J., Pitkänen, P., Puigdomenech, I., Hobbs, M., Follin, S., & Hirschorn, S., 2016: The Greenland Analogue Project: final report. *SKB Report*, TR-14-13. *Svensk Kärnbränslehantering AB*.
- Claesson Liljedahl, L., Munier, R., Sandström, B., Drake, H., & Tullborg, E.-L., 2011: Assessment of fractures classified as non-mineralised in the Sicada database. *SKB Report*, R-11-02. *Svensk Kärnbränslehantering AB*.
- Collins, S.L., Loveless, S.E., Muddu, S., Buvaneshwari, S., Palamakumbura, R.N., Krabbendam, M., Lapworth, D.J., Jackson, C. R., Gooddy, D.C., & Nara, S.N.V., 2020: Groundwater connectivity of a sheared gneiss aquifer in the Cauvery River basin, India. *Hydrogeology Journal* 28, 1371–1388.
- EngineeringToolBox, 2008: Area Moment of Inertia - Typical Cross Sections I. https://www.engineeringtoolbox.com/area-moment-inertia-d_1328.html, Accessed 07 Dec 2020.
- EngineeringToolBox, 2009: Beams - Supported at Both Ends - Continuous and Point Loads. https://www.engineeringtoolbox.com/beam-stress-deflection-d_1312.html Accessed 07 Dec 2020.
- Follin, S., Leven, J., Hartley, L., Jackson, P., Joyce, S., Roberts, D., & Swift, B., 2007: Hydrogeological characterisation and modelling of deformation zones and fracture domains, Forsmark modelling stage 2.2. *SKB Report*, R-07-48. *Svensk Kärnbränslehantering AB*.
- Forsberg, O., Mærsk Hansen, L., Koyi, S., Vestgård, J., Öhman, J., Petersson, J., Albrecht, J., Hedenström, A., & Gustavsson, J., 2007: Forsmark site investigation: detailed fracture and bedrock mapping, quaternary investigations and GPR measurements at excavated outcrop AFM001264. *SKB Report*, P-05-269. *Svensk Kärnbränslehantering AB*.
- Glamheden, R., Fredriksson, A., Roesshoff, K., Karlsson, J., Hakami, H., & Christiansson, R., 2007: Rock mechanics Forsmark. Site descriptive modelling Forsmark stage 2.2. *SKB Report TR-07-31*, *Svensk Kärnbränslehantering AB*.
- Gunnell, Y., 1998: The interaction between geological structure and global tectonics in multistoreyed landscape development: a denudation chronology of the South Indian shield. *Basin Research* 10, 281–310.
- Hall, A. & Van Boeckel, M., 2020: Origin of the Baltic Sea basin by Pleistocene glacial erosion. *GFF* 142, 237–252.
- Hall, A.M., Ebert, K., Goodfellow, B.W., Hättestrand, C., Heyman, J., Krabbendam, M., Moon, S., & Stroeven, A.P., 2019a: Past and future impact of glacial erosion in Forsmark and Uppland. *SKB Report*, TR-19-07. *Svensk Kärnbränslehantering AB*.
- Hall, A.M., Krabbendam, M., Van Boeckel, M., Ebert, K., Hättestrand, C., & Heyman, J., 2019b: The sub-Cambrian unconformity in Västergötland, Sweden: reference Surface for Glacial Erosion of Basement, Technical Report. *SKB Report*, TR-19-21. *Svensk Kärnbränslehantering AB*.
- Hall, A.M., Krabbendam, M., Van Boeckel, M., Goodfellow, B.W., Hättestrand, C., Heyman, J., Palamakumbura, R., Stroeven, A.P., & Näslund, J.-O., 2020: Glacial ripping: geomorphological evidence from Sweden for a new process of glacial erosion. *Geografiska Annaler: Series A, Physical Geography* 112, 1–21.
- Hallet, B., 1996: Glacial quarrying: a simple theoretical model. *Annals of Glaciology* 22, 1–8.
- Harper, J.T., Meierbachtol, T., & Humphrey, N.F., 2019: Greenland ICE Project, Final Report. *SKB Report*, R-18-06. *Svensk Kärnbränslehantering AB*.
- Hermanson, J., Hansen, L., Vestgård, J., & Leiner, P., 2003: Forsmark site investigation. Detailed fracture mapping of the outcrops Klubbudden, AFM001098 and Drill Site 4, AFM001097. *SKB Report*, P-03-115. *Svensk Kärnbränslehantering AB*.
- Hökmark, H. & Lönnqvist, M., 2014: Reply to comment by Christopher Talbot on “Approach to estimating the maximum depth for glacially induced hydraulic jacking in fractured crystalline rock at Forsmark, Sweden”. *Journal of Geophysical Research: Earth Surface* 119, 955–959.
- Hökmark, H., Lönnqvist, M., & Fälth, B., 2010: THM-issues in repository rock. Thermal, mechanical, thermo-mechanical and hydro-mechanical evolution of the rock at the Forsmark and Laxemar sites. *SKB Report*, TR-10-23. *Svensk Kärnbränslehantering AB*.
- Holbrook, W.S., Marcon, V., Bacon, A.R., Brantley, S.L., Carr, B.J., Flinchum, B.A., Richter, D.D., & Riebe, C.S., 2019: Links between physical and chemical weathering inferred from a 65-m-deep borehole through Earth’s critical zone. *Scientific Reports* 9, 1–11.
- Iverson, N.R., 1991: Potential effects of subglacial water-pressure fluctuations on quarrying. *Journal of Glaciology* 37, 27–36.
- Jahns, R.H., 1943: Sheet structure in granites: its origin and use as a measure of glacial erosion in New England. *The Journal of Geology* 51, 71–98.
- Japsen, P., Green, P.F., Bonow, J.M., & Erlström, M., 2016: Episodic burial and exhumation of the southern Baltic Shield: epeirogenic uplifts during and after break-up of Pangaea. *Gondwana Research* 35, 357–377.
- Lagerbäck, R., Sundh, M., Svedlund, J.-O., & Johansson, H., 2005: Searching for evidence of late- or postglacial faulting in the Forsmark region. Results from 2002–2004. *SKB Report*, P-05-51. *Svensk Kärnbränslehantering AB*.

- Leijon, B., 2005: Investigations of superficial fracturing and block displacements at drill site 5. *SKB Report*, P-05-199. *Svensk Kärnbränslehantering AB*.
- Lönnqvist, M. & Hökmark, H., 2013: Approach to estimating the maximum depth for glacially induced hydraulic jacking in fractured crystalline rock at Forsmark, Sweden. *Journal of Geophysical Research: Earth Surface* 118, 1777–1791.
- Martel, S.J., 2017: Progress in understanding sheeting joints over the past two centuries. *Journal of Structural Geology* 94, 68–86.
- Martin, C.D., 2007: Quantifying in situ stress magnitudes and orientations for Forsmark. Forsmark stage 2.2. *SKB Report*, R-07-26. *Svensk Kärnbränslehantering AB*.
- Moon, S., Perron, J.T., Martel, S.J., Goodfellow, B.W., Mas Ivars, D., Hall, A., Heyman, J., Munier, R., Näslund, J.O., & Simeonov, A., 2020: Present-day stress field influences bedrock fracture openness deep into the subsurface. *Geophysical Research Letters* 47, e2020GL090581.
- Morland, L. & Morris, E., 1977: Stress in an elastic bedrock hump due to glacier flow. *Journal of Glaciology* 18, 67–75.
- Palamakumbura, R., Krabbendam, M., Whitbread, K., & Arnhardt, C., 2020: Data acquisition by digitizing 2-D fracture networks and topographic lineaments in geographic information systems: further development and applications. *Solid Earth* 11, 1731–1746.
- Phillips, E., Everest, J., & Reeves, H., 2013: Micromorphological evidence for subglacial multiphase sedimentation and deformation during overpressurized fluid flow associated with hydrofracturing. *Boreas* 42, 395–427.
- Pusch, R., Börgesson, L., & Knutsson, S., 1990: Origin of silty fracture fillings in crystalline bedrock. *Geologiska Föreningens i Stockholm Förhandlingar* 112, 209–213.
- Robertsson, A.-M., 2004: Forsmark Site Investigation: microfossil Analyses of Till and Sediment Samples from Forsmark, Northern Uppland. *SKB Report*, P-04-110. *Svensk Kärnbränslehantering AB*.
- Sandström, B., Annersten, H., & Tullborg, E.-L., 2010: Fracture-related hydrothermal alteration of metagranitic rock and associated changes in mineralogy, geochemistry and degree of oxidation: a case study at Forsmark, central Sweden. *International Journal of Earth Sciences* 99, 1–25.
- Sandström, B., Tullborg, E., Smellie, J., MacKenzie, A., & Suksi, J., 2008: Fracture mineralogy of the Forsmark site. *SKB Report*, R-08-102. *Svensk Kärnbränslehantering AB*.
- Sandström, B. & Tullborg, E.-L., 2009: Episodic fluid migration in the Fennoscandian Shield recorded by stable isotopes, rare earth elements and fluid inclusions in fracture minerals at Forsmark, Sweden. *Chemical Geology* 266, 126–142.
- Singhal, B.B.S. & Gupta, R.P., 2010: *Applied hydrogeology of fractured rocks*. Springer Science & Business Media, Dordrecht: 408.
- Stephansson, O. & Ericsson, B., 1975: Pre-Holocene joint fillings at Forsmark, Uppland, Sweden. *Geologiska Föreningens i Stockholm Förhandlingar* 97, 91–95.
- Stephens, M.B., 2010: Forsmark site investigation. Bedrock geology – overview and excursion guide. *SKB Report*, R-10-04. *Svensk Kärnbränslehantering AB*.
- Svensk Kärnbränslehantering, 2010: Climate and climate-related issues for the safety assessment SR-Site. *SKB Report* TR-10-49. *Svensk Kärnbränslehantering AB*.
- Svensk Kärnbränslehantering, 2013: Site description of the SFR area at Forsmark at completion of the site investigation phase. *SDM-PSU Forsmark. SKB Report* TR-11-04, *Svensk Kärnbränslehantering AB*.
- Talbot, C., 1990: Problems posed to a bedrock radwaste repository by gently dipping fracture zones. *Geologiska Föreningens i Stockholm Förhandlingar* 112, 355–359.
- Talbot, C.J., 1999: Ice ages and nuclear waste isolation. *Engineering Geology* 52, 177–192.
- Talbot, C.J., 2014: Comment on “Approach to estimating the maximum depth for glacially induced hydraulic jacking in fractured crystalline rock at Forsmark, Sweden” by M. Lönnqvist and H. Hökmark. *Journal of Geophysical Research: Earth Surface* 119, 951–954.
- Twidale, C., 1973: On the origin of sheet jointing. *Rock Mechanics* 5, 163–187.
- Wright, P.J., Harper, J.T., Humphrey, N.F., & Meierbachtol, T.W., 2016: Measured basal water pressure variability of the western Greenland Ice Sheet: implications for hydraulic potential. *Journal of Geophysical Research: Earth Surface* 121, 1134–1147.
- Ziegler, M., Loew, S., & Moore, J.R., 2013: Distribution and inferred age of exfoliation joints in the Aar Granite of the central Swiss Alps and relationship to Quaternary landscape evolution. *Geomorphology* 201, 344–362.
- Zoet, L., Alley, R.B., Anandakrishnan, S., & Christianson, K., 2013: Accelerated subglacial erosion in response to stick-slip motion. *Geology* 41, 159–162.

Appendix

Equation derivation

The problem equates to the structural engineering problem of a beam supported at both ends under a uniform continuous, distributed load. The maximum stress that such a beam is subjected to (compressive at the top, and tensional at the base of the beam) is given by (EngineeringToolBox 2009):

$$\sigma_{max} = Y_{max}qL^2/8I \quad [1a]$$

where Y_{max} is $\frac{1}{2}$ height of beam, so that:

$$\sigma_{max} = 0.5h_rqL^2/8I \quad [1b]$$

where h_r is the height of the beam, L the length of the beam, q_{tot} is the total load and I is the Area Moment of Inertia. The Area Moment of Inertia I for a rectangular cross-section is given by (EngineeringToolBox 2008):

$$I = wh_r^3/12 \quad [2]$$

So that (taking width $w = 1$):

$$\sigma_{max} = \frac{0.5hq_{tot}L^2 \cdot 12}{8wh_r^3} \text{ or: } \sigma_{max} = \frac{0.75q_{tot}L^2}{h_r^3} \quad [3]$$

The load is the sum of the load of the overlying rock and the ice, minus the water pressure at the base:

$$q_{tot} = q_r + q_i - P_w \text{ or: } q_{tot} = gh_r\rho_r + gh_i\rho_i - P_w \quad [4]$$

where q_{tot} is the total load, q_r is the load exerted by the rock beam itself, q_i the load of the overlying ice, P_w the water pressure, g the gravity constant, h_i the thickness of the ice and ρ_i and ρ_r the density of ice and rock respectively.

It is convenient to express this in terms of relative water pressure (P_w/P_i). Because:

$$P_i - P_w = P_i(1 - P_w/P_i) \text{ and: } P_i = gh_i\rho_i$$

the total load can also be written as:

$$q_{tot} = gh_r\rho_r + P_i\left(1 - \frac{P_w}{P_i}\right) \text{ or} \quad [5]$$

Combining equation [3] and [5], the maximum stress at the base of a rock beam as a function of the height and length of the beam and ice thickness and relative water pressure is given by:

$$\sigma_{max} = \frac{0.75\left[gh_r\rho_r + gh_i\rho_i\left(1 - \frac{P_w}{P_i}\right)\right]L^2}{h_r^3} \quad [6]$$

The maximum length of the beam can then be given as:

$$L = h_r\sqrt{\sigma_{max}/\left(0.75\left(gh_r\rho_r + gh_i\rho_i\left(1 - \frac{P_w}{P_i}\right)\right)\right)} \quad [7]$$

σ_{max} = maximum stress (Pa or N/m²)

q_{tot} total load; q_r : load by overlying rock; q_i : load by overlying ice; (all in Pa)

I : Moment of inertia (m⁴)

L : length of beam (m) w : width of beam (taken as 1 m) h_r : height of beam (m)

h_i : height of ice (m)

ρ_r : density of rock (2800 kg/m³)

ρ_i : density of ice (910 kg/m³)

P_w : water pressure (in Pa)